DOI: 10.26599/FSHW.2025.9250901

Contents lists available at SciOpen

Food Science and Human Wellness

journal homepage: https://www.sciopen.com/journal/2097-0765

China Food Publishing Co.

Cordycepin Attenuates Microglial-Mediated Neurotoxicity in Alzheimer's Disease Through Dual Modulation of Pro-Inflammatory and Phagocytic Functions via Caspase1 Suppression and STAT6 Activation

Ke Du[a1], Benyu Su[a1], Chunhong Jin[b1], Juan Wang[a1], Luoxuan Su[a], Xi Zheng[a,d*], Ying Duan[c*], Mingyan Liu[a*]

[a]*School of Pharmacy, Department of Pharmacology, China Medical University, Shenyang, 110001, Liaoning, China*

[b]*Department of Health, Yuncheng Vocational and Technical University, Yuncheng, 044000, China*

[c]*Liaoning Maternal and Child Health Hospital, Shenyang, 110001, China*

[d]*Pharmacy Department, Chongqing Emergency Medical Center, Chongqing University Central Hospital, Medical College, Chongqing University, Chongqing, 400014, China*

ABSTRACT: Microglia (MG) play dual roles in Alzheimer's disease (AD) development. They can worsen the condition by causing inflammation but also help in early stages by removing harmful amyloid-beta (Aβ) through phagocytosis. Consequently, precise modulation of microglial phagocytic activity and inflammatory responses holds considerable significance for AD treatment. Cordycepin (Cor) is a representative active component extracted from Cordyceps militaris, which is a type of medicinal and nutritional food. Although Cor is considered to exert neuroprotective effects, its potential regulatory role in microglial function in AD, as well as the underlying specific mechanisms, remain poorly elucidated. Through transcriptomics combined with *in vitro* and *in vivo* experimental validations, we demonstrated that Cor suppresses the pro-inflammatory responses of MG while enhancing their phagocytic capacity for Aβ, with these dual effects mediated through distinct mechanisms. Specifically, on one hand, Cor can activate the STAT6 signaling pathway to upregulate the expression of phagocytosis-related factors, including Arg1, TGFβ, IL10, and CD206, thereby promoting the clearance of Aβ by MG. Notably, activation of the STAT6 signaling pathway does not affect the inflammatory response. On the other hand, Cor can inhibit caspase1 to reduce the levels of inflammation-related factors such as IL1β, TNFα, iNOS, and CD86, thereby alleviating neuroinflammation. Meanwhile, inhibition of caspase1 activity does not impact phagocytic function. This unique dual action of Cor, which simultaneously suppresses inflammation and promotes phagocytosis of MG, opens new avenues for prevention and therapeutic strategies against AD and provides solid experimental evidence and theoretical support.

1. Introduction

Microglia (MG) are the macrophages of the central nervous system (CNS) and display neurotoxic or neuroprotective functions depending upon their pro-inflammatory or phagocytic functions, thereby acting as a double-edged sword in neurological disease[1, 2]. Pro-inflammatory phenotype macrophages are considered to enhance inflammatory responses by secreting large numbers of destructive pro-inflammatory mediators such

[1]These authors contributed equally to this work and share first authorship.
***Corresponding author**
Mingyan Liu, liumy_cmu@163.com; Ying Duan, duanying1333@163.com; Xi Zheng, zx601377036@outlook.com

Received 24 January 2025
Received in revised from 6 March 2025
Accepted 3 April 2025

as interleukin 1β (IL1β), tumor necrosis factor α (TNFα), and expressing inducible nitric oxide synthase (iNOS), thereby accelerating cytotoxicity and tissue damage[3]. On the other hand, phagocytic macrophages clear apoptotic cell debris and toxic proteins such as amyloid-beta (Aβ), while upregulating both anti-inflammatory factors and phagocytosis-related factors, such as interleukin 10 (IL10), transforming growth factor β (TGFβ), arginase 1 (Arg1), and CD206, to promote inflammation resolution and tissue repair[4, 5].

In the early stages of Alzheimer's disease (AD), MG exert neuroprotective effects by phagocytosing various harmful substances, including Aβ aggregates and apoptotic cellular debris, thereby clearing toxic materials and suppressing inflammation[2, 6]. However, as AD progresses, the sustained production of Aβ overwhelms the phagocytic capacity of MG. This leads to a persistent pro-inflammatory phenotype and chronic neuroinflammation, which disrupts CNS homeostasis and ultimately contributes to neuronal damage[7]. Therefore, the regulation of microglial function from pro-inflammatory phenotype to phagocytic phenotype should be expected as an outstanding therapeutic and preventive approach for AD treatment.

Cordyceps militaris is highly valued as traditional tonic medicine and food in Asian countries[8-10]. Cordycepin (Cor), as the main active constituent from *Cordyceps militaris*, has been reported to have various pharmacological activities, including anti-inflammation, anti-angiogenesis, anti-tumor and anti-proliferation[10-13]. In addition, accumulating evidence suggested that Cor is able to protect CNS neurons in conditions such as stroke or reperfusion injury[14-16]. It has been also reported that Cor could inhibit Aβ-induced apoptosis and neuronal hyperactivity in vitro-cultured hippocampal neurons[17, 18], suggesting its therapeutic potential in the treatment of AD. Recently, we have also demonstrated that Cor mediates neuroprotection by regulating microglial nerve growth factor (NGF) expression and mitochondrial metabolic reprogramming in AD models[19, 20]. In this study, we further found that Cor not only suppresses MG-mediated neuroinflammation but also enhances phagocytic function at the same time, through a novel dual mechanism involving caspase1 suppression and STAT6 activation, respectively. These findings provide new evidence for the therapeutic potential of Cor and offer fresh insights for AD treatment strategies.

2. Materials and methods

2.1. Materials

Cell culture reagents were purchased from Gibco (USA). Cor, $A\beta_{1-42}$ (Aβ), LPS and Z-YVAD were purchased from Sigma-Aldrich (USA). AS1517499 was purchased from Selleckchem (China).

2.2. Cell culture

The immortalized murine microglial cell line BV2 and human neuro-blastoma cell line SH-SY5Y were purchased from the Institute of Basic Medical Sciences of Chinese Academy of Medical Sciences (China). BV2 and SH-SY5Y cells were cultured in Dulbecco's modified Eagle's medium (DMEM) and DMEM/Eagle's medium and Ham's F-12 (F12) respectively, supplemented with 10% fetal bovine serum (FBS) and 100

units/mL of penicillin-streptomycin in a 37℃, 5% CO_2 incubator. Cells at passage 8-20 were used for the experiments.

2.3. Conditioned culture and CCK8 assay

BV2 cells were cultured in 6-well plates at a density of 2×10^5 cells/well for 24 h. Then, cells were treated with or without Cor (0.6 μg/mL) for 1 h, followed by stimulation with $A\beta_{1\text{-}42}$ (40 μM) and LPS (1 μg/mL) for 6 h or not. The supernatant was replaced with fresh medium and cultured for another 24 h. Then, collected the microglia-conditioned media.

SH-SY5Y cells were cultured in 96-well plates at a density of 1×10^3 cells/well and cultured for 24 h, then replaced the media with the microglia-conditioned media and cultured for another 24 h. Finally, CCK-8 reagents (10 μL/well) were added and incubated at 37℃ for 2 h, and the absorbance at 450 nm was detected to calculate the cell viability by a multi-mode reader (LD942, Beijing, China).

2.4. RNA-seq library construction and sequencing

The cDNA libraries were constructed and sequenced by Metware Biotechnology Co., Ltd. (Wuhan, China) using the Illumina sequencing platform. A total of six samples were subjected to transcriptome sequencing (RNA-seq). BV2 cells were treated with or without Cor (0.6 μg/mL) for 1 hour, followed by stimulation with Aβ1-42 (10 μM) and LPS (1 μg/mL) for 6 hours. Each treatment condition included three biological replicates. First, poly(A)-tailed mRNA was enriched using Oligo(dT) magnetic beads and fragmented into short segments using fragmentation buffer. Double-stranded cDNA was then synthesized using random hexamer primers, followed by end repair, A-tailing, and adapter ligation. The cDNA libraries were amplified by PCR and subjected to rigorous quality control, including RNA integrity assessment (RIN≥8) and library fragment size verification. Finally, paired-end sequencing (PE150) was performed, with each sample yielding at least 7 Gb of clean data and a Q30 base percentage ≥ 97%, ensuring high data reliability.

2.5. Real-time RT-PCR

Total RNA was isolated from BV2 cells with TRIzol reagent (CWBIO) according to the manufacturer's instructions. Next, RNA was reverse-transcribed to complementary DNA using the Prime Script RT-PCR Kit (Takara) primed with oligo(dT). Quantitative real-time PCR was carried out using the SYBR Green PCR Mix Kit (Takara). The primer sequences were as follows: IL1β:5′-TCGCAGCAGCACATCAACAAGAG -3′ (forward) and 5′-TGCTCATGTCCTCATCCTGGAAGG -3′ (reverse); TNFα: 5′-AGCCCACGTCGTAGCAAACCAC -3′ (forward) and 5′- AGGTACAACCCATCGGCTGGCA -3′ (reverse); iNOS: 5′- CCTTGGTGAAGGGACTGAGC -3′ (forward) and 5′-CAACGTTCTCCGTTCTCTTGC -3′ (reverse); Arg1: 5′- AGGCTGTGGTTGGTAGAGGTGATC -3′ (forward) and 5′- ACTGTGTTCGCTGTGACTGTTGG -3′ (reverse); TGFβ: 5′-GCAACAATTCCTGGCGTTACCTTG -3′ (forward) and 5′- CAGCCACTGCCGTACAACTCC -3′ (reverse); IL10: 5′- AGGCAGTGGAGCAGGTGAAGAG -3′ (forward) and 5′-

TCTAACTGGCAGAGGAGGTCACAC -3′ (reverse); GAPDH: 5′- AGCCTCGTCCCGTAGACAAAA-3′ (forward) and 5′- TGGCAACAATCTCCACTTTGC-3′ (reverse). Relative quantification of mRNA levels compared to the internal housekeeping gene GAPDH was calculated. The data were analyzed using the relative gene expression changes ($2^{-\Delta\Delta}$Ct) method for quantification.

2.6. Phagocytosis assay

For live-cell imaging experiments, BV2 cells were plated at a density of 2×10^5 cells per well in confocal dishes and cultured for 24 hours. Experimental groups were pretreated with 1 μg/mL Cor for 1 hour prior to incubation with 250 nmol/L HiLyte Fluor™ 488-labeled β-amyloid (1-42) (488-Aβ; AnaSpec, Inc., USA), while control groups received 488-Aβ treatment only. Images were captured every 30 minutes for 12 hours using a live cell imaging microscope (Zeiss, Germany) and analyzed by ImageJ (Fiji) software. After channel separation to identify 488-Aβ localization, integrated density (IntDen) was measured to quantify the amount of 488-Aβ phagocytosed by microglial cells. This IntDen was then divided by the number of microglial cells in the field of view for normalization.

2.7. Fluorescence-activated cell sorting (FACS)

As described previously, BV2 microglial cells were seeded at a density of 2×10^5 cells/well in 6-well plates and cultured for 24 hours under standard conditions (37°C, 5% CO_2). Following a 12-hour incubation with 488-Aβ (250 nmol/L), cells were gently detached by pipetting and collected by centrifugation at 1,500 r/min for 5 minutes. After three washes with 1 mL PBS to remove non-phagocytosed 488-Aβ aggregates, the MG

population was resuspended in 0.4 mL PBS. Fluorescence-activated cell sorting was then performed using the FACS Celesta flow cytometer (BD, USA) to isolate 488-$A\beta^+$ microglial cells.

2.8. Animals and treatment

As described before, all animal care and experimental procedures were in compliance with the Standard Medical Laboratory Animals' Care and Use Protocols (Ministry of Health PR China, 1998) and the Laboratory Animal Ethical Standards of China Medical University (KT2022403).

Seven-month-old APP/PS1 transgenic mice were randomly assigned into two groups (n=5 per group): Cor-treated APP/PS1 group (APP/PS1 + Cor group) and vehicle-treated APP/PS1 group (APP/PS1 group). Five age-matched wild-type C57BL/6 mice were assigned as control group (WT group, n=5). Cor was dissolved in distilled water at a concentration of 1 mg/mL. Mice in the Cor-treated APP/PS1 group were administered by gavage with 40 mg · kg^{-1} · day^{-1} Cor (diluted in distilled water) for 4 weeks, and mice in the APP/PS1 and WT groups received the same volume of distilled water (vehicle control). These mice were euthanized after behavioral tests.

2.9. Passive avoidance test

After 4 weeks of the Cor treatment, mice were subjected to a passive avoidance test (PAT), as previously described. The apparatus (BA-200, Taimeng Technology Co., Ltd. (Chengdu, China)) was divided into two

compartments, including a lighted compartment and a darkened one, and they were connected by an automatic guillotine door. The dark compartment was equipped with a grid floor placed through which a foot-shock can be delivered. Mice underwent two independent trials: a training session and a test session conducted 24 hours later. In the training session, the mice were placed in the light compartment for 3 min of habituation. Then, the guillotine door was opened to allow the mice to enter the dark compartment. As soon as the mice entered the dark compartment, the guillotine door was closed and a mild electrical foot shock (0.5 mA) was delivered for 2 seconds. In the test session, each mouse was reevaluated in a similar manner. However, a foot-shock was not delivered, and the latencies and frequencies for mice to enter the dark compartment were recorded for up to 300 seconds.

2.10. Morris Water Maze Test

After the PAT, the mice were given Morris water maze (MWM) test for consecutive 7 days and the protocol used in this study was obtained from previous reports[21, 22]. The MWM was conducted using a stainless-steel circular water tank (120 cm in diameter and 50 cm in height). A platform (10 cm diameter) was placed in the second quadrant and submerged 0.5 cm below the water surface. On the baseline day (day 0), mice underwent swimming for 1 minute in the pool without the platform to familiarize them with the circumstances. On training days (from the first day to the fifth day), the platform was placed under the water and the mice were subjected 60 seconds for spatial acquisition during 4 trials per day. Different starting positions were used for each trial. If a mouse did not find the platform within 60 seconds, it would be guided to the platform for 60 seconds. For each trial, the escape latency and the path length by the mouse to find the hidden platform were recorded. On the sixth day, a probe trial was conducted to assess memory consolidation. The platform was removed from the maze, and the animals were allowed to undergo free swimming for 60 seconds. The frequency that each mouse crossed over the former platform location and the percentage of time that each mouse spent in the quadrant were monitored. All the data were obtained by a video tracking system (MWT-100; Taimeng Technology Co., Ltd. (Chengdu, China)).

2.11. Western blotting

As described before, to obtain brain tissues, the mice in each group were euthanized by decapitation, and the brains were rapidly removed. The brains were then cut into left and right hemispheres, and the cerebral cortex was dissected out and used for western blotting. For BV2 cells, they were pretreated with or without Cor (0.6 μg/ml), Z-YVAD (5 μM) and AS1517499 (50 nmol/L) for 1 h, followed by stimulation with $A\beta_{1\text{-}42}$ (10 μm) and LPS (1 μg/ml) for 6 h. Then, the brain tissues and BV2 cells were homogenized on ice for 1 h in precooling RIPA lysis buffer (Beyotime, China) containing a protease inhibitor cocktail (Sigma-Aldrich, USA). The lysates were then centrifuged at 12 000 *g* for 30 min at 4 ℃. The supernatants were collected, and protein qualification was carried out using a BCA kit (Beyotime, China). Proteins (30 μg) were separated on SDS-polyacrylamide gels, and transferred to a polyvinylidene difluoride membrane (Millipore, CA). The membrane was incubated with TBS containing 0.1% Tween-20 (TBST) with 5% bovine serum albumin for 1 h, followed by incubation with rabbit anti-mouse polyclonal primary antibodies against IL1β (1:1000, CST),

TNFα (1:1000, CST), Arg1 (1:1000, CST), TGFβ (1:1000, CST), IL18 (1:1000, Abcam), caspase1 (CASP1) (1:1000, CST), STAT6 (1:1000, CST), Phospho-STAT6 (1:1000, CST) and β-actin (1:1000, Santa Cruz) overnight at 4 ℃. After washing with TBST for 3 times, the membranes were probed with HRP-conjugated secondary antibodies (1:5000; Santa Cruz) for 1 h at room temperature. Finally, immunoreactive bands were visualized using an enhanced chemiluminescent kit (ECL+, Amersham Biosciences) and were analyzed using the Quality One analysis software (BioRad). The relative expression of target proteins was normalized to β-actin.

2.12. Immunofluorescence

Immunofluorescence analysis was performed as previously described[22]. Briefly, paraffin-embedded slices of cerebral cortex tissues (4 μm) were blocked with 5% BSA in PBS for 1 hour at room temperature followed by an overnight incubation at 4℃ with rabbit anti-mouse primary antibody against Iba1 (1:500, Abcam), and goat anti-mouse primary antibodies against CD86 (1:500, R&D Systems) or CD206(1:500, R&D Systems). Then, the slices were washed with PBS and incubated with FITC-conjugated goat anti-rabbit IgG and TRITC-conjugated rabbit anti-goat IgG secondary antibody (1:200, Invitrogen) for 1 hour at 37 ℃ in the dark. Nuclear staining was performed using DAPI (Sigma-Aldrich) for 5 min at room temperature. After washing with PBS for 3 times, the immunofluorescence images were subsequently acquired using a confocal laser scanning microscope (Nikon).

2.13. Statistical analysis

Statistical analyses were performed using SPSS (Statistical Package for the Social Sciences, version 13.0). The data are presented as mean ± SD. Differences among groups were determined by one-way analysis of variance followed by Tukey's post hoc test. $P < 0.05$ was considered to be statistically significant.

3. Results

3.1. Cor inhibits pro-inflammatory function and enhances phagocytic activity of MG in $A\beta_{LPS}$-treated BV2 cells

To investigate the functional regulation and the underlying molecular mechanisms of Cor on MG in AD, we performed transcriptome sequencing on microglial cells from both the Aβ+LPS ($A\beta_{LPS}$) treated model group and the Cor-treated $A\beta_{LPS}$ group. We conducted a heatmap analysis and found that, compared to the model group, pro-inflammatory factors, such as IL1β, TNF, and IL6, etc., generally showed a downregulation trend after Cor treatment. Conversely, compared to the model group, phagocytosis-promoting genes (like IL10, TGFβ2, and CX3CL1, etc.) showed an up-regulation trend after Cor treatment, while phagocytosis-inhibiting genes, such as CD33, Sirpb1c, and Siglece, exhibited the down-regulation pattern (Fig. 1A). Further, KEGG analysis identified key pathways associated with the differentially expressed genes between the $A\beta_{LPS}$ treated model group and the Cor-treated $A\beta_{LPS}$ group, including JAK-STAT signaling pathway, cytokine-cytokine receptor interaction, TNF signaling pathway, etc. (Fig. 1B), Most of them were associated with the regulation of pro-inflammatory or phagocytic states of MG. Therefore, we further

confirmed the impacts of Cor on pro-inflammatory / phagocytic phenotypic function in $A\beta_{LPS}$-treated BV2 cells. The results demonstrated that Cor significantly suppressed the mRNA levels of pro-inflammatory mediators (IL1β, TNFα, and iNOS) ($^{*}P < 0.05$, $^{**}P < 0.01$; Fig. 1C) and increased the mRNA levels of phagocytosis-related molecules (Arg1, TGFβ, and IL10) ($P < 0.01$; Fig. 1D). Quantitative live-cell imaging analysis further revealed that, compared to MG treated with 488-Aβ alone, those treated with Cor showed a progressive enhancement in their phagocytic capacity towards 488-Aβ over a 12-hour period. This finding indicates that Cor significantly augments the phagocytosis of 488-Aβ on MG ($P < 0.01$; Fig. 1E and F; Additional file 1 and 2). Consistent with the mRNA expression profiles, the protein levels of IL1β and TNFα were also decreased ($P < 0.01$; Fig. 1G, H and S1), whereas the protein levels of Arg1 and TGFβ were increased in Cor-treated group ($P < 0.01$; Fig. 1G and H). To further validate whether Cor's modulation of microglial function affects Aβ-induced neurotoxicity, conditioned culture and CCK-8 assay were conducted and the results showed that microglial conditioned media from $A\beta_{LPS}$-induced BV2 cells significantly decreased the cell viability of SH-SY5Y cells treated by Aβ ($P < 0.01$; Fig. 1I), whereas the decline was reversed after Cor pre-treatment on $A\beta_{LPS}$-induced BV2 cells ($P < 0.01$; Fig. 1I). These results suggested that Cor exerts neuroprotective effects in AD by regulating functional transformation of MG.

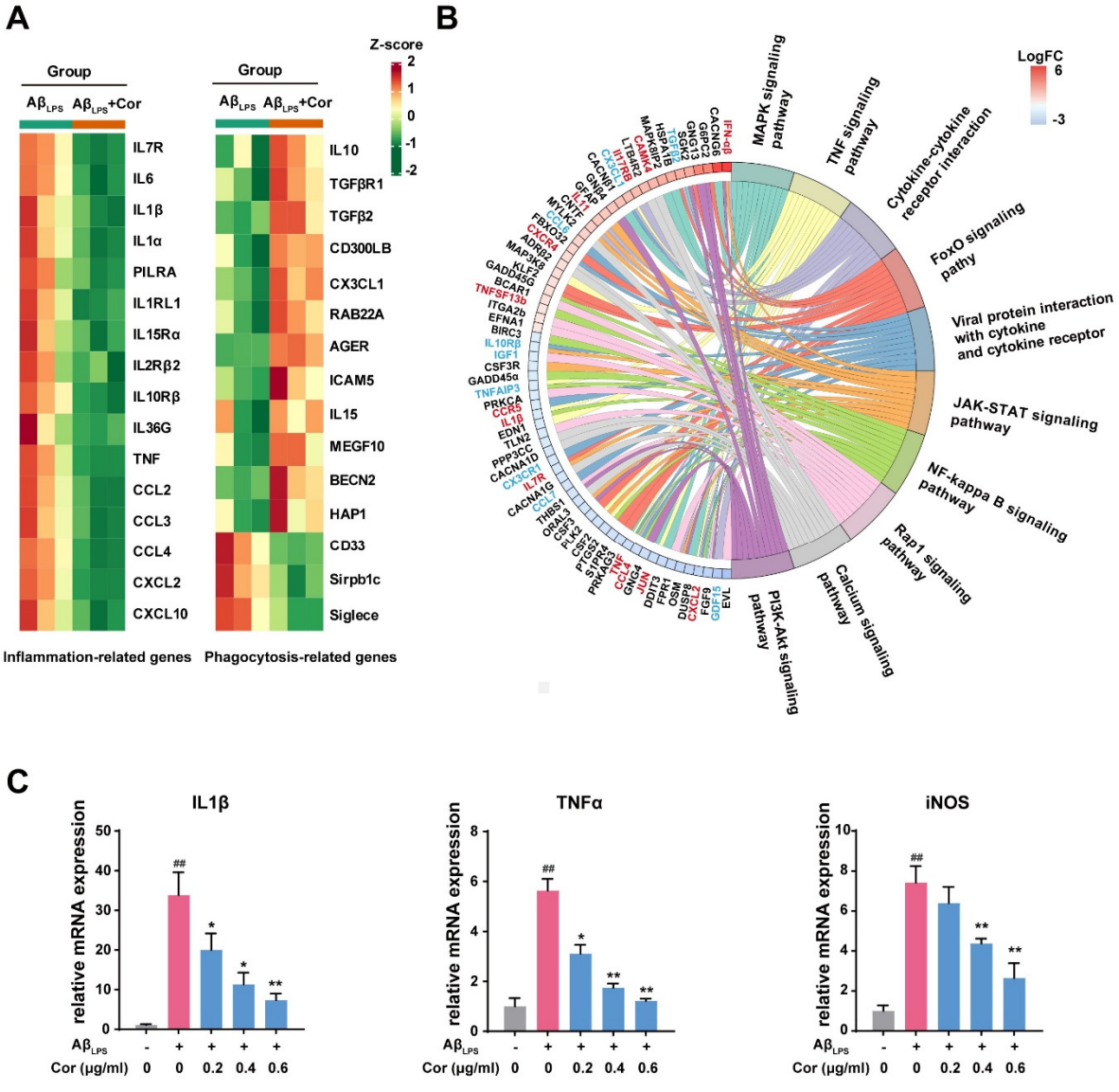

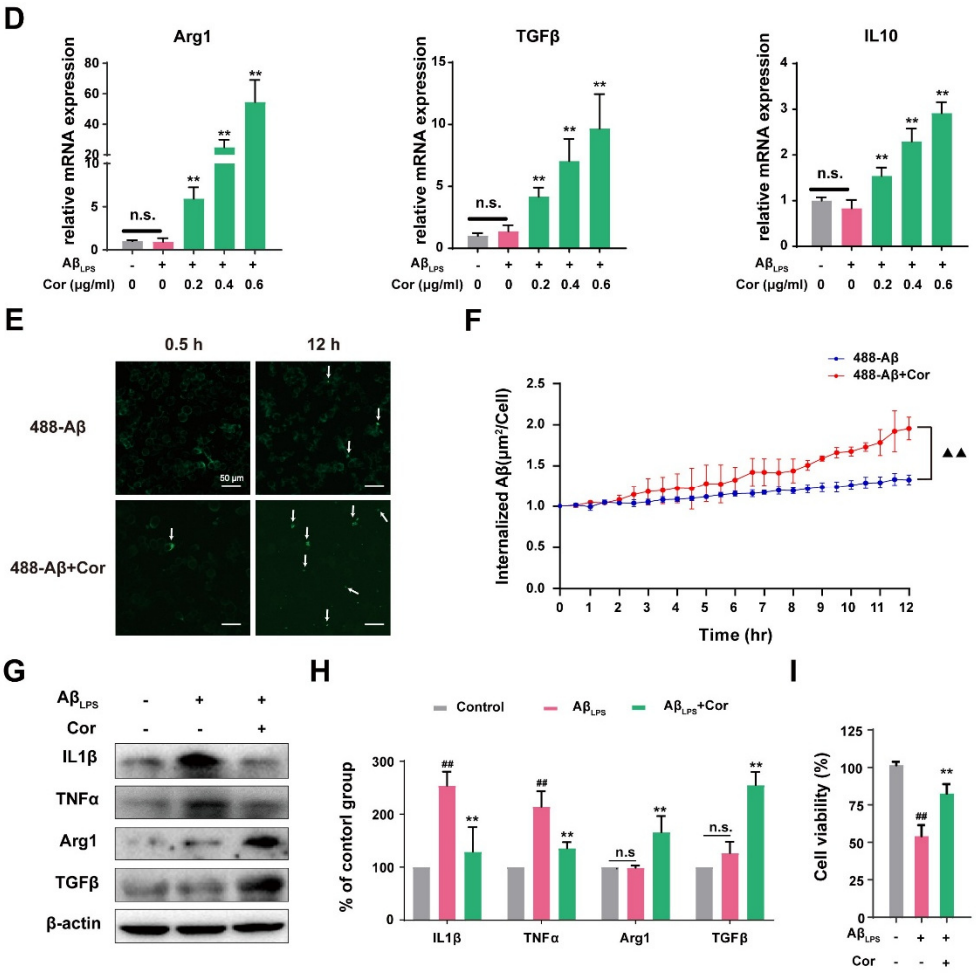

Figure 1. Effects of Cor on the regulation of microglial function and neurotoxicity in vitro. (A) Heatmap analysis of inflammation-related genes and phagocytosis-related genes in the $A\beta_{LPS}$-treated model group versus the Cor-treated $A\beta_{LPS}$ group. The heatmap data were derived from transcriptome sequencing, normalized by Z-score transformation, with color intensity representing the standard deviation multiples of gene expression relative to the mean. (B) Gene-pathway association string diagram showing the association between DEGs and enriched KEGG pathway. The red indicates inflammation-related genes, and the blue indicates phagocytosis-related genes. (C and D) BV2 cells were pretreated with or without Cor (0.2, 0.4, 0.6 μg/ml) for 1 h, followed by stimulation with $A\beta_{1\text{-}42}$ (40 μM) and LPS (1 μg/ml) for 6 h. The mRNA levels of pro-inflammatory factors (IL1β, TNFα, iNOS) and phagocytosis-associated factors (Arg1, TGFβ and IL10) were analyzed by real-time PCR assay. (E and F) BV2 cells were pretreated with or without Cor (0.6 μg/ml) for 1 h and stimulated with 488-Aβ (250 nm). Images were collected at 15 min intervals for 12h under the live cell imaging microscope. Bar = 50 μm. All images were analyzed by imageJ software. Internalized Aβ = IntDen/BV2 cell number. (G and H) BV2 cells were pretreated without or with Cor (0.6 μg/ml) for 1 h, followed by stimulation with $A\beta_{1\text{-}42}$ (40 μM) and LPS (1 μg/ml) for 6 h. The protein levels of IL1β, TNFα, Arg1 and TGFβ were evaluated by western blot. The relative protein expression levels of the above proteins were normalized to actin. (I) BV2 cells were pretreated without or with Cor (0.6 μg/ml) for 1 h, followed by stimulation with $A\beta_{1\text{-}42}$ (40 μM) and LPS (1 μg/ml) for 6 h. Replace the supernatant with new media and culture for 24 h. Then, SH-SY5Y cells were treated with the MG-conditioned media for 24 h. Cell viability of SH-SY5Y cells was assessed by CCK-8 assay. All assays were performed in triplicate. Values are mean ± SD (n=3). One-way analysis of variance followed by Tukey's post hoc test was used to analyze the statistical differences. $^{\#}P < 0.05$, $^{\#\#}P < 0.01$, vs vehicle group; $^{*}P < 0.05$, $^{**}P < 0.01$, vs $A\beta_{LPS}$-treated group; $^{\blacktriangle}P < 0.05$, $^{\blacktriangle\blacktriangle}P < 0.01$, vs 488-Aβ group.

3.2. STAT6 activation is involved in Cor-induced MG phagocytic phenotype in $A\beta_{LPS}$-treated BV2 cells

As indicated by KEGG enrichment results, the JAK–STAT pathway attracted our attention. STAT6 (signal transducer and activator of transcription 6), a key protein in the JAK-STAT pathway, has drawn significant research attention due to its ability to reduce pro-inflammatory cytokine production and enhance macrophage phagocytic function upon activation[23-26]. Therefore, we then investigated whether the activation of STAT6 was involved in Cor-induced MG transition from pro-inflammatory to phagocytic phenotype.

Western blot results showed that Cor treatment significantly increased the expression of phosphorylated STAT6 (p-STAT6) in $A\beta_{LPS}$-treated BV2 cells ($P < 0.05$; Fig. 2A and B). After the exposure to STAT6 inhibitor AS1517499, the up-expression of phagocytosis-related factors induced by Cor were significantly decreased ($^{*}P < 0.05$, $^{**}P < 0.01$; Fig. 2C-F), whereas there was no significant change in pro-inflammatory factors both at mRNA (Fig. 2C and D) and protein levels (Fig. 3E and F). Furthermore, we used the live cell imaging microscope to observe the MG and performed flow cytometry on the 488-Aβ group and the 488-Aβ group co-treated with Cor. We found that the phagocytosis efficiency of BV2 cells for 488-Aβ was enhanced after Cor treatment for 12 h ($P < 0.05$; Fig. 2G-I). While, this effect was inhibited by the STAT6 inhibitor AS1517499 ($P < 0.01$; Fig. 2G-I). These results demonstrated that Cor can activate STAT6, and this activation is associated with its ability to promote microglial phagocytosis of Aβ, but not with its inhibitory effect on neuroinflammation.

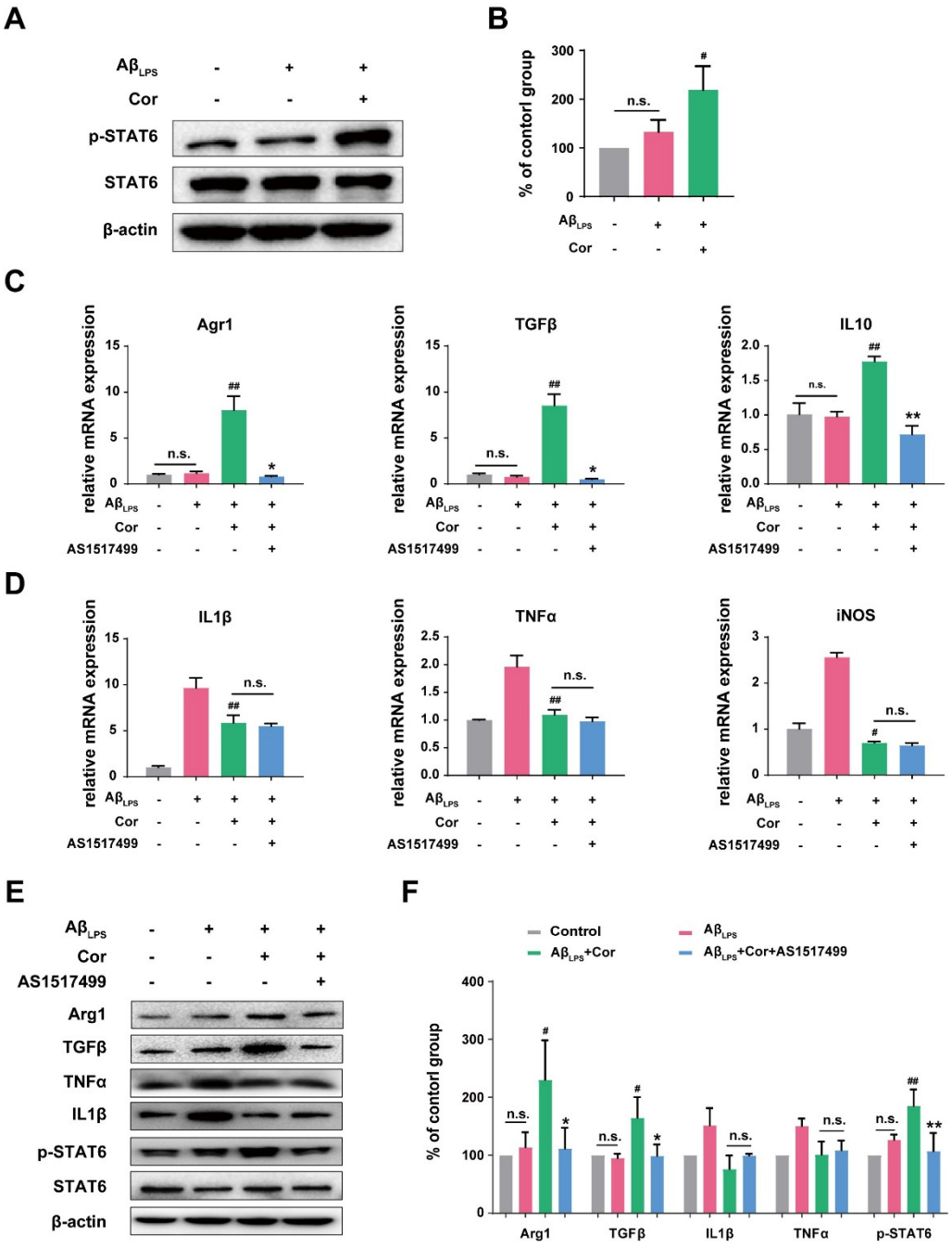

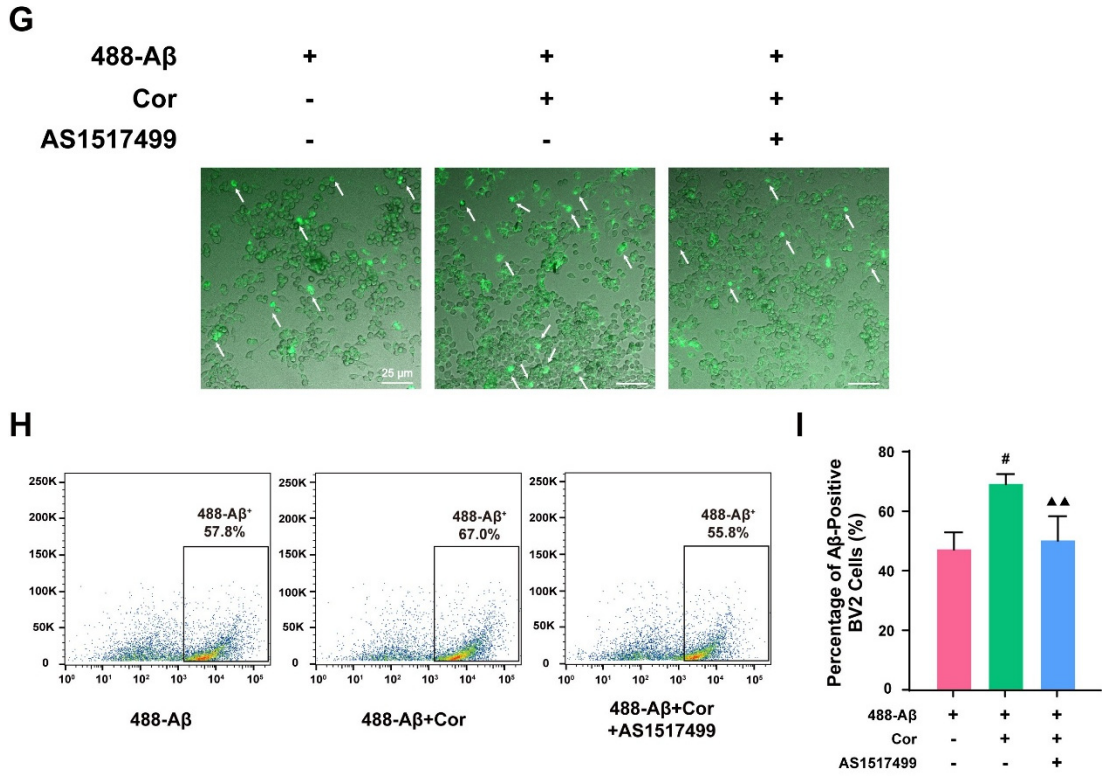

Figure 2. Effects of Cor on STAT6-dependent phagocytic phenotype MG activation in $A\beta_{LPS}$-treated BV2 cells. BV2 cells were pretreated with or without Cor (0.6 μg/ml) and AS1517499 (50 nmol/L) for 1 h, followed by stimulation with $A\beta_{1\text{-}42}$ (40 μM) and LPS (1 μg/ ml) for 6 h. (A and B) The protein levels of p-STAT6 and STAT6 were analyzed by western blot. The relative expression levels of p-STAT6 were normalized to STAT6. (C and D) The mRNA levels of pro-inflammatory factors (IL1β, TNFα, iNOS) and phagocytosis-associated factors (Arg1, TGFβ and IL10) were analyzed by real-time PCR assay. (E and F) The protein levels of IL1β, TNFα, Arg1, TGFβ were evaluated by western blot. The relative protein expression levels were normalized to actin. The relative expression levels of p-STAT6 were normalized to STAT6. (G) Images captured by the live cell imaging microscope before flow cytometry, showing the effects of Cor treatment on the phagocytic capacity of BV2 cells for 488-Aβ, as well as the effect of the STAT6 inhibitor AS1517499 on the phagocytic ability of BV2 cells. Bar = 25 μm. (H and I) The phagocytic capacity of flow cytometry-sorted BV2 cells for 488-Aβ, and the effect of the STAT6 inhibitor AS1517499 on the phagocytic ability of BV2 cells. All the experiments were performed in triplicate. Values are mean ± SD (n=3). One-way analysis of variance followed by Tukey's post hoc test was used to analyze statistical differences. $^{\#}P < 0.05$, $^{\#\#}P < 0.01$, vs $A\beta_{LPS}$-treated group or vs 488-Aβ group; $^{*}P < 0.05$, $^{**}P < 0.01$, vs $A\beta_{LPS}$+Cor group; $^{\blacktriangle}P < 0.05$, $^{\blacktriangle\blacktriangle}P < 0.01$, vs 488-Aβ+Cor group.

3.3. Cor inhibited pro-inflammatory phenotype of MG in $A\beta_{LPS}$-treated BV2 cells via inhibiting caspase1 activation

Aberrant activation of the NLRP3 inflammasome is critically involved in MG-mediated pro-inflammatory responses in AD[27], with caspase1 acting as the central mediator[28, 29]. Therefore, we then investigated whether the regulatory effect of Cor on microglial pro-inflammatory was related to caspase1. The results showed that $A\beta_{LPS}$ treatment increased the levels of caspase1, as well as those of its downstream factors, IL1β and IL18($P < 0.05$; Fig. 3A and B). However, Cor treatment significantly reversed these effects ($^{*}P < 0.05$, $^{**}P < 0.01$; Fig. 3A and B). These results suggest that Cor can suppress caspase1 activation. To further investigate whether the inhibitory effect of Cor on caspase1 affects the pro-inflammatory and phagocytic functions of MG, we treated BV2 cells with caspase1 inhibitor Z-YVAD and found that Z-YVAD reversed the mRNA expression of pro-inflammatory factors (IL1β, TNFα and iNOS) induced by $A\beta_{LPS}$ treatment ($^{*}P < 0.05$, $^{**}P < 0.01$; Fig. 3C), whereas it had no significant effect on mRNA expression of phagocytosis-related factors (Arg1, TGFβ and IL10) (Fig. 3D). Western blot analysis of these protein levels

was consistent with the results of RT-PCR after Z-YVAD treatment ($^{*}P < 0.05$, $^{**}P < 0.01$; Fig. 3E and F). Before the flow cytometry test, we observed MG using the live cell imaging microscope and found that Cor treatment increased the phagocytosis efficiency of BV2 cells for 488-Aβ. Moreover, adding the caspase1 inhibitor Z-YVAD did not affect this phagocytosis (Fig. 3G). The flow cytometry results confirmed these observations, further verifying that Cor enhances the phagocytosis of 488-Aβ by BV2 cells ($P < 0.05$; Fig. 3H and I), while caspase1 inhibitor Z-YVAD does not alter the phagocytosis induced by Cor (Fig. 3H and I). The findings demonstrated that Cor can suppresses the pro-inflammatory function of MG in AD by inhibiting caspase1 activation. Notably, this inhibitory effect on caspase1 does not affect the phagocytic function of MG toward Aβ.

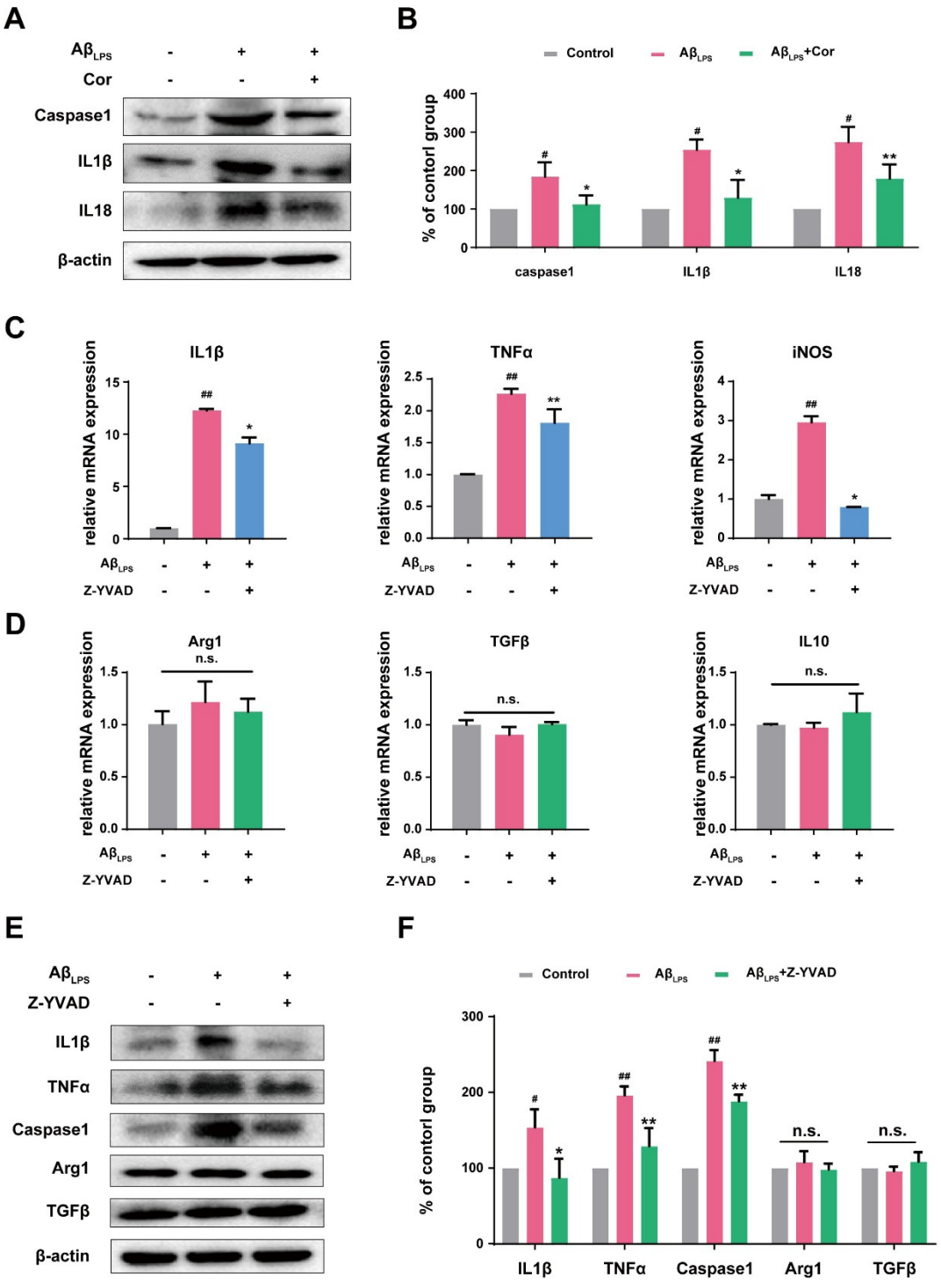

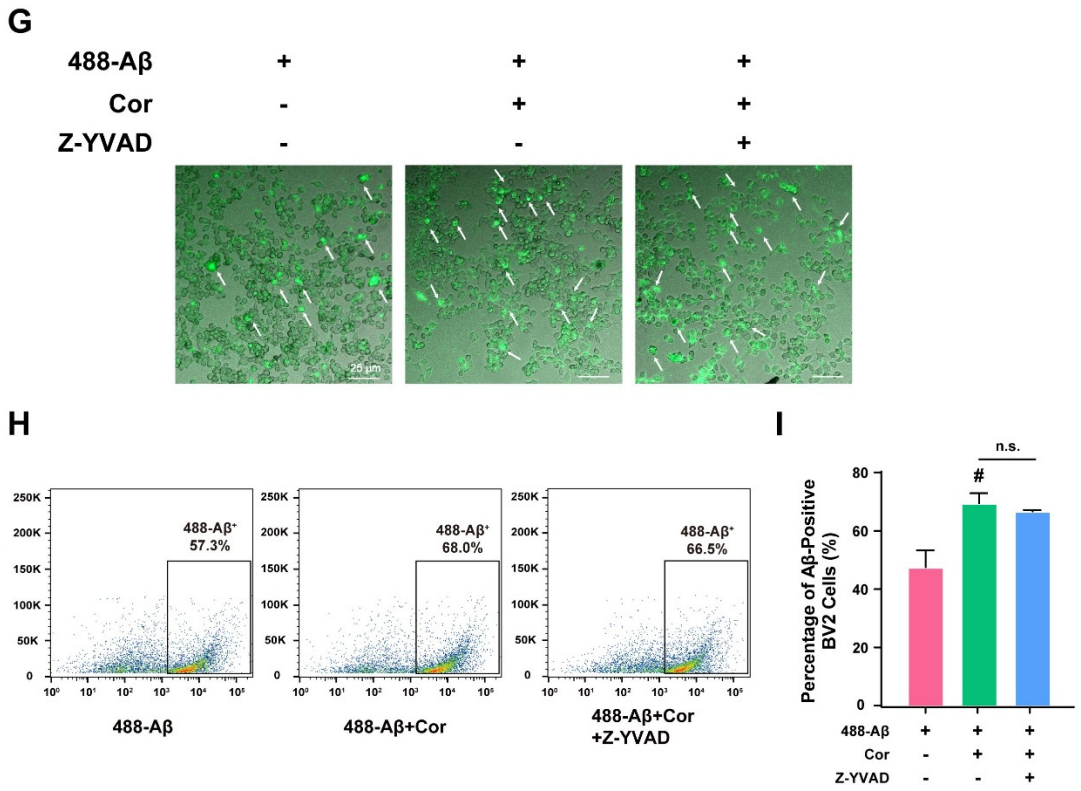

Figure 3. Effects of Cor against caspase1-dependent pro-inflammatory phenotype MG activation in $A\beta_{LPS}$-treated BV2 cells. BV2 cells were pretreated with Cor (0.6 μg/ml) or Z-YVAD (5 μM) for 1 h, followed by stimulation with $A\beta_{1-42}$ (40 μM) and LPS (1 μg/ml) for 6 h. (A and B) The protein levels of caspase1, IL1β and IL18 were analyzed by western blot. The relative expression levels of the above proteins were normalized to actin. (C and D) The mRNA levels of pro-inflammatory factors (IL1β, TNFα, iNOS) and phagocytosis-associated factors (Arg1, TGFβ and IL10) were analyzed by real-time PCR assay. (E and F) The protein levels of IL1β, TNFα, Arg1, TGFβ and caspase1 were evaluated by western blot. The relative protein expression levels of the above proteins were normalized to actin. (G) Images captured by the live cell imaging microscope before flow cytometry, showing the effects of Cor treatment on the phagocytic capacity of BV2 cells for 488-Aβ, as well as the effect of the inhibitor Z-YVAD on the phagocytic ability of BV2 cells. (H and I) The phagocytic capacity of flow cytometry-sorted BV2 cells for 488-Aβ, and the effect of the inhibitor Z-YVAD on the phagocytic ability of BV2 cells. All the experiments were performed in triplicate. Values are mean ± SD (n=3). One-way analysis of variance followed by Tukey's post hoc test was used to analyze statistical differences. $^{\#}P < 0.05$, $^{\#\#}P < 0.01$, vs vehicle group or vs 488-Aβ group; $^{*}P < 0.05$, $^{**}P < 0.01$, vs $A\beta_{LPS}$-treated group.

3.4. Cor treatment ameliorated learning and memory deficits in APP/PS1 mice

In vitro experiments confirmed that Cor exerts anti-AD toxic effects through two distinct mechanisms: it promotes microglial phagocytosis by activating the STAT6 pathway, while simultaneously suppressing microglial inflammatory responses by inhibiting caspase1. Subsequently, we validated this neuroprotective effect of Cor and its related mechanisms in APP/PS1 transgenic AD mouse models. First, we systematically evaluated the impact of Cor on the behavioral phenotypes of these AD model mice. After Cor treatment, mice were subjected to PAT to assess their retention of nonspatial memory. The findings indicated that the APP/PS1 mice showed a decreased latency ($P < 0.05$; Fig. 4A) and an increased frequency ($P < 0.01$; Fig. 4B) of entering the dark compartment compared with WT group. While, the latency to enter the dark compartment was apparently increased ($P < 0.05$; Fig. 4A) and the frequency ($P < 0.05$; Fig. 4B) of entering the dark compartment was markedly decreased in the Cor-treated APP/PS1 group.

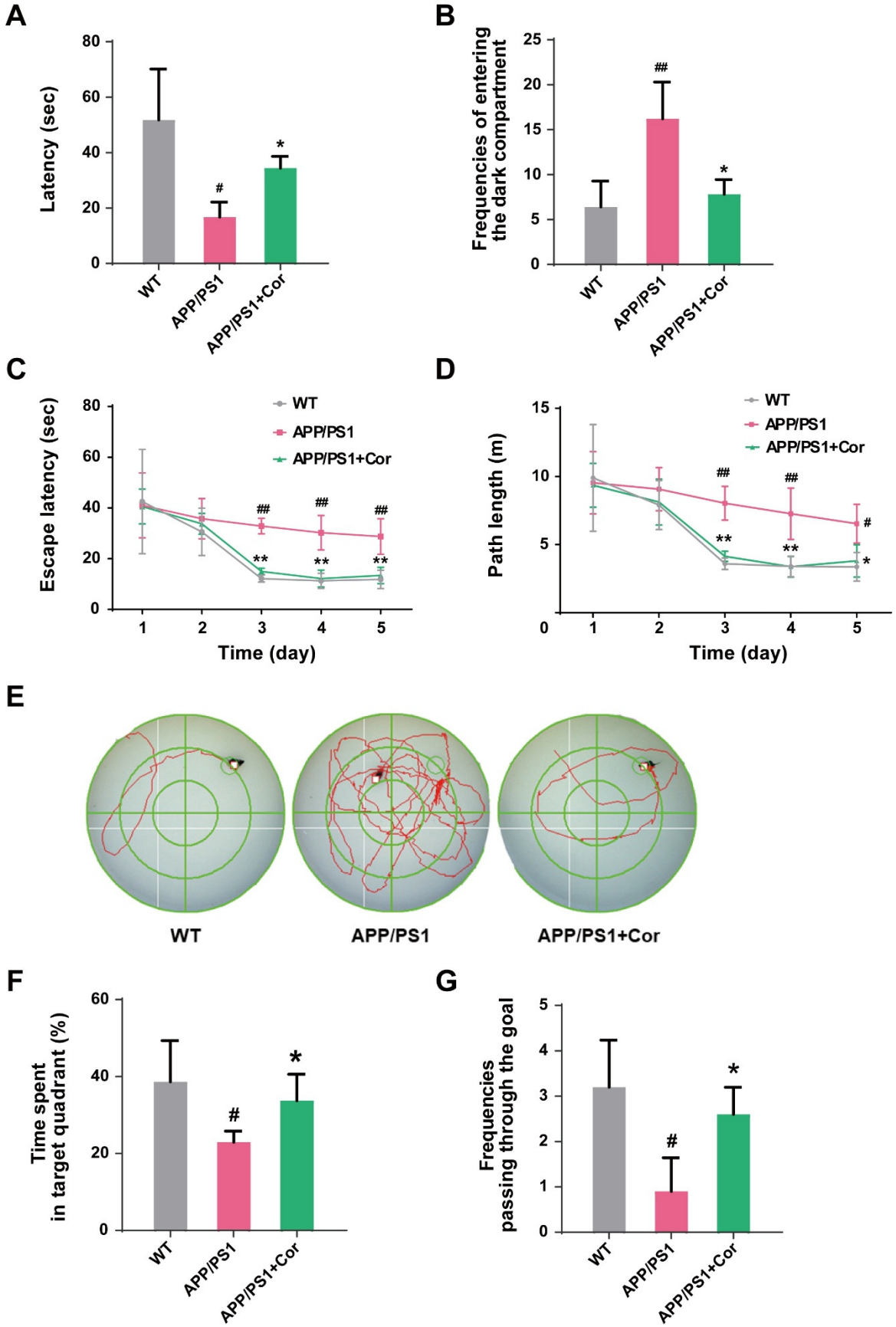

Figure 4. Effects of Cor against learning and memory deficits of APP/PS1 mice. (A and B) The latency and the frequency of entering the dark compartment of APP/PS1 mice during the passive avoidance test. (C and D) The escape latency and path length of APP/PS1 mice in the navigation test of morris water maze test. (E) The representative locus plot in the probe trial. (F and G) The time spent in target quadrant and the frequency of passing through the original platform position during the probe trial. Values are mean ± SD (n = 5). One-way analysis of variance followed by Tukey's post hoc test was used to analyze the statistical differences. $^{\#}P < 0.05$, $^{\#\#}P < 0.01$, vs wild-type (WT) group; $^{*}P < 0.05$, $^{**}P < 0.01$, vs APP/PS1 group.

After the PAT, MWM test was conducted. During navigation testing, there were no significant differences in escape latency and path length among the WT, APP/PS1, and Cor-treated APP/PS1 groups on 1-2 days (Fig. 4C-D), indicating that the motility and vision of mice were not affected in MWM test. During the following days (from the third day to the fifth day), compared to WT group, the APP/PS1 group had significantly longer escape latency ($P < 0.01$; Fig. 4C) and path length ($^{\#}P < 0.05$, $^{\#\#}P < 0.01$; Fig. 4C). While the escape latency and path length in the Cor-treated APP/PS1 group were apparently improved compared with those in the APP/PS1 mice group ($^{*}P < 0.05$, $^{**}P < 0.01$; Fig. 4C and D). Moreover, in the probe trial on the sixth day, the APP/PS1 group showed a significantly shorter swimming time in the target quadrant and crossed the original platform position fewer times ($P < 0.05$; Fig. 4E-G). While the Cor-treated APP/PS1 group spent more time in the target quadrant and showed higher frequency of crossing the original platform than those in the APP/PS1 group ($P < 0.05$; Fig. 4E-G). Further, compared with WT group, APP/PS1 mice showed darker hippocampal staining, sparse neurons, reduced Nissl bodies, and obvious vacuolization, while Cor treatment improved these deficits (Fig. S2). These results indicated that Cor can improve macroscopic brain pathological changes and ameliorate learning and memory cognitive deficits in APP/PS1 mice.

3.5. Cor suppressed pro-inflammatory phenotype and increased phagocytic phenotype of MG in the cortex of APP/PS1 mice via caspase1 inhibition and STAT6 activation, respectively

The immunofluorescence results indicated that co-localization of Iba1(MG maker) and CD86 (a pro-inflammatory macrophage marker) was observed in the cortical of APP/PS1 mice, suggesting the presence of pro-inflammatory phenotype MG activation in APP/PS1 mice (Fig. 5A). While Cor treatment reduced the co-localization of Iba1 and CD86 (Fig. 5A). In contrast, compared with the APP/PS1 group, Cor treatment increased the co-localization of Iba1 and CD206 (a phagocytic macrophage marker) (Fig. 5B). Western blot analysis showed that compared with the APP/PS1 group, the protein levels of pro-inflammatory factors (IL1β and TNFα) were apparently decreased ($P < 0.05$; Fig. 5C and D), whereas the protein levels of phagocytic-related factors (Arg1 and TGFβ) were markedly elevated in the cortical of Cor-treated APP/PS1 mice ($^{*}P < 0.05$, $^{**}P < 0.01$; Fig. 5C and D). These findings demonstrated that Cor can attenuate the activation of MG with a pro-inflammatory phenotype and enhanced its phagocytic function in the cortex of APP/PS1 mice. In accordance with our findings in vitro (Fig. 2A-B and Fig. 3A-B), Cor significantly decreased the expression levels of caspase1 ($P < 0.01$; Fig. 5E and F) and increased the expression levels of p-STAT6 ($P < 0.05$; Fig. 5E and F). These results suggested that Cor attenuated pro-inflammatory phenotype and promoted phagocytic phenotype of MG in the cortex of APP/PS1 mice, probably via caspase1- and STAT6-dependent manner.

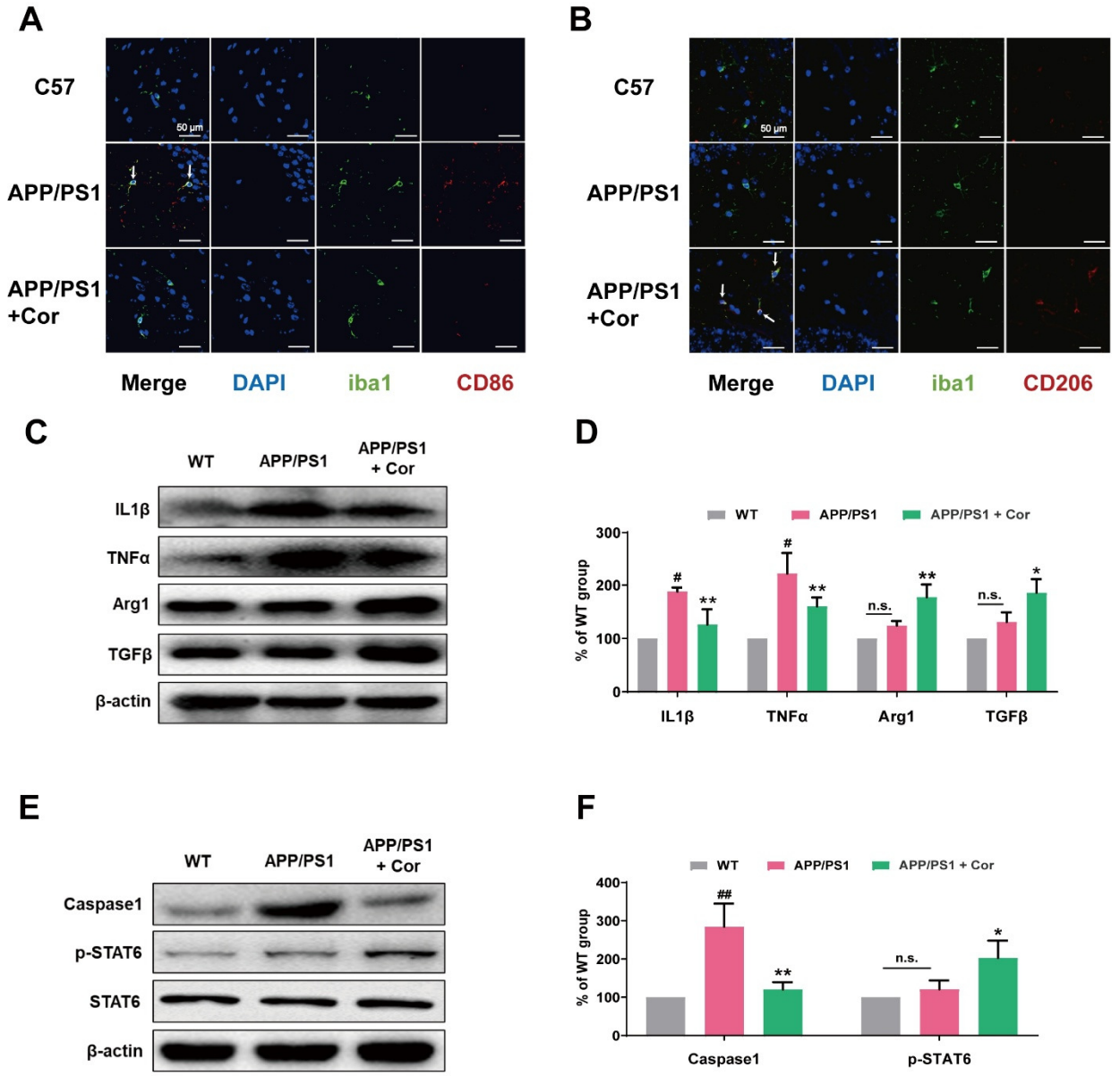

Figure 5. Effects of Cor on MG function transition via a caspase1- and STAT6-dependent manner in the cortex of APP/PS1 mice. (A and B) The localization of CD86 and Iba1, as well as CD206 and Iba1 in the cortex of APP/PS1 mice were analyzed by immunofluorescence respectively. Bar = 25 μm; (C-F) The expression levels of IL1β, TNFα, Arg1, TGFβ, caspase1, p-STAT6 and STAT6 in the cortex of APP/PS1 mice were evaluated by Western blot. The relative protein expression levels were normalized to β-actin. The relative expression levels of p-STAT6 were normalized to STAT6. Values are mean ± SD (n=3). One-way analysis of variance followed by Tukey's post hoc test was used to analyze the statistical differences. $^{\#}P < 0.05$, $^{\#\#}P < 0.01$, vs WT group; $^{*}P < 0.05$, $^{**}P < 0.01$, vs APP/PS1 group.

4. Discussion

In the current study, we found that Cor attenuates microglial activation toward a pro-inflammatory phenotype and promotes phagocytic functional transition in both APP/PS1 mice and $A\beta_{LPS}$-treated BV2 cells, thereby reducing neuronal damage. A key advantage lies in the fact that, in the presence of Aβ, Cor can directly block microglial inflammatory damage responses by inhibiting caspase1. Meanwhile, it can also promote microglial phagocytosis and clearance of Aβ through activating STAT6, thereby fundamentally eliminating the source of inflammatory stimulation. This dual regulatory mechanism confers potential synergistic and additive benefits of Cor in the treatment of AD.

Previous research has also shown that parthenolide (PTL) can inhibit neuroinflammation by activating Tripartite Motif Containing 31 and suppressing NLRP3 inflammasome activation, while also enhancing microglial phagocytosis through the AKT/MAPK/NF-κB pathway to promote Aβ clearance and improve cognitive function in APP/PS1 mice[30]. Additionally, Jo et al. reported that Gossypetin enhances phagocytosis by MG and reduces neuroinflammation, thereby improving Aβ deposition and cognitive function in 5 × FAD mice[31]. Although these studies differ from ours in terms of the drugs, mechanisms, and AD models employed, they all support a novel and promising therapeutic strategy for AD. This strategy exerts neuroprotective effects on neurons in AD by bidirectionally regulating the pro-inflammatory and phagocytic functions of MG, thereby modifying the neuroimmune microenvironment.

Phagocytosis is a key function of MG, regulated by multiple signaling pathways. Among them, the JAK-STAT signaling pathway plays an important role in modulating phagocytosis, with STAT6 being a crucial factor within this pathway. Activation of STAT6 significantly upregulates the expression of phagocytic phenotype-related factors, such as Arg1, TGFβ, and IL10, thereby enhancing the phagocytic function of MG[32-34]. Previous studies have shown that IL4 may enhance microglial phagocytic function by activating the STAT6 pathway, thereby alleviating neuroinflammation following intracerebral hemorrhage[35]. Another study demonstrated that resveratrol can activate STAT6, reduce nerve damage, and promote the transformation of phagocytic function of MG in LPS-induced inflammatory models[36]. Consistent with previous research findings, we confirmed in this study that Cor can activate STAT6 in both BV2 cells and AD mouse models. Moreover, the use of the STAT6 inhibitor AS1517499 reversed the enhanced phagocytic function of MG induced by Cor in $A\beta_{LPS}$-treated BV2 cells, suggesting that Cor enhances the phagocytic function of MG through STAT6 activation. However, our results indicate that the activation of STAT6 does not regulate inflammatory responses, despite other studies suggesting an association between STAT6 and inflammatory responses. This discrepancy may be attributed to differences in disease conditions, experimental models, and the drugs used across various studies.

Caspase1 is the main component of the NLRP3 inflammasome. Caspase1-mediated NLRP3 inflammasome activation triggers multiple signaling cascades that upregulate inflammatory mediators such as IL1β, IL18, TNFα and IL6, thereby amplifying neuroinflammation and creating a self-perpetuating vicious cycle of neuronal damage[37, 38]. Our previous studies demonstrated that both baicalin and epigallocatechin-3-gallate attenuated MG-mediated neuroinflammation by suppressing caspase1-mediated NLRP3 inflammasome in AD models[6, 22]. In this study, we also found that the activation of caspase1 and its downstream effectors IL1β/IL18 was significantly increased after $A\beta_{LPS}$ treatment in vitro and in the cortex of APP/PS1 mice in vivo. Notably, Cor administration effectively reversed these effects. Consistent with the effect of Cor, treatment with Z-YVAD (a specific inhibitor of Caspase1) also significantly alleviated the inflammatory response in $A\beta_{LPS}$-treated group. However, we found that the caspase1 specific inhibitor Z-YVAD showed no significant effects on the phagocytic function of BV2 cells. Therefore, we conclude that

Cor exerts anti-inflammatory effects through caspase1 inhibition, and its mechanism appears independent of phagocytic function enhancement.

In addition, our study has several limitations. To date, the FDA has only approved eight drugs for treating Alzheimer's symptoms. These include two anti-amyloid drugs (aducanumab and lecanemab), four cholinesterase inhibitors (donepezil, tacrine, galantamine, and rivastigmine), one NMDA receptor antagonist (memantine), and the combination of donepezil and memantine. We found that the mechanism underlying anti-AD effect of Cor is associated with its anti-inflammatory activity and promotion of microglial phagocytosis of Aβ. Notably, the therapeutic mechanisms of these positive agents differ from those of Cor, so it is challenging to identify a suitable positive drug in the mechanistic studies. Second, we selected the BV2 cell line as the experimental model for the following reasons. It is an immortalized microglial cell line that is readily available and can provide a stable and sufficient supply of cells, facilitating large-scale and repeatable experiments. Moreover, we selected the BV2 cell line as the experimental model for the following reasons. BV2 cell line is an immortalized microglial cell line that is readily available and can provide a stable and sufficient supply of cells, facilitating large-scale and repeatable experiments. Moreover, BV2 cell line retains the fundamental characteristics of microglial cells, making it an effective model for studying their functions and mechanisms. However, we are also aware of the limitations of using only the BV2 cell line. Compared with primary human microglia, the BV2 cell line may have potential differences. Primary human microglia and microglia derived from human induced pluripotent stem cells (iPSC) more closely resemble the human physiological state in terms of cell receptor expression, protein secretion, cellular functions, and response characteristics. These cells can provide more comprehensive experimental data for the role of Cor in treating AD. Therefore, it is necessary to employ a broader range of cell models to further elucidate the mechanisms of Cor. Third, we found that the dosage of Cor used in pharmacological studies ranges from 2 mg/kg to 72 mg/kg in mice across various previously established disease models [39]. Therefore, we ultimately selected a dose of 40 mg/kg for the formal animal experiment in this study and found that a favorable therapeutic effect is achieved at this concentration. However, it is necessary to establish multiple concentration gradients in animal experiments and further expand the dosage range of Cor in future studies.

Within the scope of our literature search, no reports on Cor-related research involving human subjects have been identified. However, existing research has confirmed that Cor can cross the BBB in mouse models[40]. Additionally, studies in mice and rats have shown that Cor exhibits low bioavailability, which can be improved by co-administering Cor metabolic inhibitors, synthesizing Cor derivatives with enhanced stability, or applying novel drug delivery systems[41]. Based on the animal dose (40 mg/kg) in this study, the human equivalent dose of Cor is estimated to be 3.24 mg/kg using allometric scaling normalized to body surface area. An acute toxicity study of Cor in mice demonstrated that intraperitoneal administration of Cor at a dose of 3600 mg/kg/d (equivalent to 291.9 mg/kg/d in humans) for 14 consecutive days exerted no significant effects on the body weight or major organs of normal mice[42]. Therefore, we hypothesize that the human equivalent dose corresponding to the Cor dosage administered to mice in this study is likely to be safe

for humans. However, the specific therapeutic dosage and efficacy of Cor in humans remain to be elucidated through further research.

In conclusion, Cor, which is the main active component extracted from *Cordyceps militaris*, exerts neuroprotective effects by inhibiting the pro-inflammatory phenotype and enhancing the phagocytic function of MG, with mechanisms involving caspase1 inhibition and STAT6 activation (Fig. 6). These findings also suggest that functional foods based on Cor hold promise as a potent means for neuroprotection in AD.

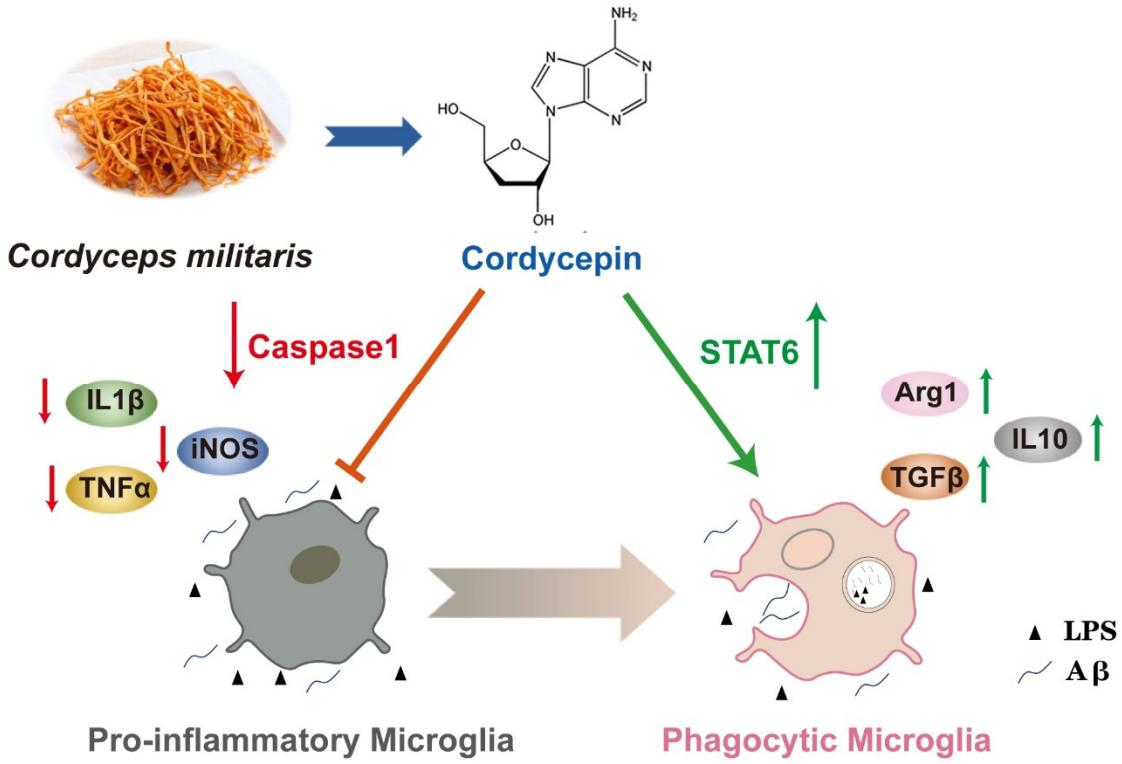

Figure 6. Cordycepin from *Cordyceps militaris* exerts anti-AD neurotoxicity by inhibiting microglial inflammation via caspase1 inhibition and promoting phagocytosis via STAT6 activation.

Ethics approval and consent to participate

Ethical approval for this study was approved by the Institutional Ethics Review Boards of China Medical University (KT2022403) and all experiments were performed in accordance with ARRIVE guidelines (https://arriveguidelines.org) and the Laboratory Animal Ethical Standards of China Medical University.

Declaration of competing interest

The authors declare that they have no known competing financial interests or personal relationships that could have appeared to influence the work reported in this paper.

Acknowledgements

This work was supported by Natural Science Foundation of Liaoning Province (JYTMS20230129 and 2024-MS-025), Basic Scientific Research Project of Institutions of Higher Learning of Liaoning Province (No. LJKZ0775), the Joint Plan of Science and Technology of Liaoning Province (2023-MSLH-369), and Yuncheng Vocational and Technical University (KY2022-2-2). We are grateful to Wuhan Metware Biotechnology Co., Ltd for assisting in sequencing and bioinformatics analysis. The authors would like to

thank all the reviewers who participated in the review and MJEditor (www.mjeditor.com) for their linguistic assistance in preparing this manuscript.

Data Availability Statement

The data supporting the findings of this study are available from the corresponding authors upon reasonable request.

References

[1] K. Yao, H.B. Zu, Microglial polarization: novel therapeutic mechanism against Alzheimer's disease, Inflammopharmacology, 28 (2020) 95-110. https://doi.org/10.1007/s10787-019-00613-5.

[2] X. Jin, M.Y. Liu, D.F. Zhang, et al., Natural products as a potential modulator of microglial polarization in neurodegenerative diseases, Pharmacol Res, 145 (2019) 104253. https://doi.org/10.1016/j.phrs.2019.104253.

[3] Y. Tang, W. Le, Differential Roles of M1 and M2 Microglia in Neurodegenerative Diseases, Mol Neurobiol, 53 (2016) 1181-94. https://doi.org/10.1007/s12035-014-9070-5.

[4] D. Boche, C. Cunningham, F. Docagne, et al., TGFbeta1 regulates the inflammatory response during chronic neurodegeneration, Neurobiol Dis, 22 (2006) 638-50. https://doi.org/10.1016/j.nbd.2006.01.004.

[5] R. Orihuela, C.A. McPherson, G.J. Harry, Microglial M1/M2 polarization and metabolic states, Br J Pharmacol, 173 (2016) 649-65. https://doi.org/10.1111/bph.13139.

[6] X. Zhong, M. Liu, W. Yao, et al., Epigallocatechin-3-Gallate Attenuates Microglial Inflammation and Neurotoxicity by Suppressing the Activation of Canonical and Noncanonical Inflammasome via TLR4/NF-kappaB Pathway, Mol Nutr Food Res, 63 (2019) e1801230. https://doi.org/10.1002/mnfr.201801230.

[7] G. Ma, M. Liu, K. Du, et al., Differential Expression of mRNAs in the Brain Tissues of Patients with Alzheimer's Disease Based on GEO Expression Profile and Its Clinical Significance, Biomed Res Int, 2019 (2019) 8179145. https://doi.org/10.1155/2019/8179145.

[8] B. Cong, Perspectives in Food & Medicine Homology, Food & Medicine Homology, 1 (2024) 9420018. https://doi.org/10.26599/FMH.2024.9420018.

[9] S.K. Law, D.C.T. Au, A review of medicine and food homology on traditional Chinese medicine as functional food, Food & Medicine Homology;10.26599/FMH.2026.9420091(2025) https://doi.org/10.26599/FMH.2026.9420091.

[10] O.J. Olatunji, J. Tang, A. Tola, et al., The genus Cordyceps: An extensive review of its traditional uses, phytochemistry and pharmacology, Fitoterapia, 129 (2018) 293-316. https://doi.org/10.1016/j.fitote.2018.05.010.

[11] K.J. Won, S.C. Lee, C.K. Lee, et al., Cordycepin attenuates neointimal formation by inhibiting reactive oxygen species-mediated responses in vascular smooth muscle cells in rats, J Pharmacol Sci, 109 (2009) 403-12. https://doi.org/10.1254/jphs.08308fp.

[12] Y.T. Lin, S.M. Liang, Y.J. Wu, et al., Cordycepin Suppresses Endothelial Cell Proliferation, Migration, Angiogenesis, and Tumor Growth by Regulating Focal Adhesion Kinase and p53, Cancers (Basel), 11 (2019) https://doi.org/10.3390/cancers11020168.

[13] P. Hu, W. Chen, J. Bao, et al., Cordycepin modulates inflammatory and catabolic gene expression in interleukin-1beta-induced human chondrocytes from advanced-stage osteoarthritis: an in vitro study, Int J Clin Exp Pathol, 7 (2014) 6575-84. https://www.ncbi.nlm.nih.gov/pubmed/25400736

[14] Z. Cheng, W. He, X. Zhou, et al., Cordycepin protects against cerebral ischemia/reperfusion injury in vivo and in vitro, Eur J Pharmacol, 664 (2011) 20-8. https://doi.org/10.1016/j.ejphar.2011.04.052.

[15] K. Takakura, S. Ito, J. Sonoda, et al., Cordyceps militaris improves the survival of Dahl salt-sensitive hypertensive rats possibly via influences of mitochondria and autophagy functions, Heliyon, 3 (2017) e00462. https://doi.org/10.1016/j.heliyon.2017.e00462.

[16] L.H. Yao, C.H. Li, W.W. Yan, et al., Cordycepin decreases activity of hippocampal CA1 pyramidal neuron through membrane hyperpolarization, Neurosci Lett, 503 (2011) 256-60. https://doi.org/10.1016/j.neulet.2011.08.048.

[17] H. Song, L.P. Huang, Y. Li, et al., Neuroprotective effects of cordycepin inhibit Abeta-induced apoptosis in hippocampal neurons, Neurotoxicology, 68 (2018) 73-80. https://doi.org/10.1016/j.neuro.2018.07.008.

[18] L.H. Yao, J. Wang, C. Liu, et al., Cordycepin protects against beta-amyloid and ibotenic acid-induced hippocampal CA1 pyramidal neuronal hyperactivity, Korean J Physiol Pharmacol, 23 (2019) 483-91. https://doi.org/10.4196/kjpp.2019.23.6.483.

[19] X. Zhong, S. Gong, L. Meng, et al., Cordycepin Modulates Microglial M2 Polarization Coupled with Mitochondrial Metabolic Reprogramming by Targeting HKII and PDK2, Adv Sci (Weinh), 11 (2024) e2304687. https://doi.org/10.1002/advs.202304687.

[20] L. Jiao, Z. Yu, X. Zhong, et al., Cordycepin improved neuronal synaptic plasticity through CREB-induced NGF upregulation driven by MG-M2 polarization: a microglia-neuron symphony in AD, Biomed Pharmacother, 157 (2023) 114054. https://doi.org/10.1016/j.biopha.2022.114054.

[21] M. Liu, F. Chen, L. Sha, et al., (-)-Epigallocatechin-3-gallate ameliorates learning and memory deficits by adjusting the balance of TrkA/p75NTR signaling in APP/PS1 transgenic mice, Mol Neurobiol, 49 (2014) 1350-63. https://doi.org/10.1007/s12035-013-8608-2.

[22] X. Jin, M.Y. Liu, D.F. Zhang, et al., Baicalin mitigates cognitive impairment and protects neurons from microglia-mediated neuroinflammation via suppressing NLRP3 inflammasomes and TLR4/NF-kappaB signaling pathway, CNS Neurosci Ther, 25 (2019) 575-90. https://doi.org/10.1111/cns.13086.

[23] T. Lawrence, G. Natoli, Transcriptional regulation of macrophage polarization: enabling diversity with identity, Nat Rev Immunol, 11 (2011) 750-61. https://doi.org/10.1038/nri3088.

[24] W. Cai, X. Dai, J. Chen, et al., STAT6/Arg1 promotes microglia/macrophage efferocytosis and inflammation resolution in stroke mice, JCI Insight, 4 (2019) https://doi.org/10.1172/jci.insight.131355.

[25] J. Xu, Z. Chen, F. Yu, et al., IL-4/STAT6 signaling facilitates innate hematoma resolution and neurological recovery after hemorrhagic stroke in mice, Proc Natl Acad Sci U S A, 117 (2020) 32679-90. https://doi.org/10.1073/pnas.2018497117.

[26] Q. Shen, L. Zhao, L. Pan, et al., Soluble SIRP-Alpha Promotes Murine Acute Lung Injury Through Suppressing Macrophage Phagocytosis, Front Immunol, 13 (2022) 865579. https://doi.org/10.3389/fimmu.2022.865579.

[27] Y. Gao, S. Li, Y. Zhang, et al., Cattle Encephalon Glycoside and Ignotin Attenuates Abeta1-42-Mediated Neurotoxicity by Preventing NLRP3 Inflammasome Activation and Modulating Microglial Polarization via TLR4/NF-kappaB Signaling Pathway, Neurotox Res, 40 (2022) 1802-11. https://doi.org/10.1007/s12640-022-00585-5.

[28] J. Flores, A. Noel, B. Foveau, et al., Caspase-1 inhibition alleviates cognitive impairment and neuropathology in an Alzheimer's disease mouse model, Nat Commun, 9 (2018) 3916. https://doi.org/10.1038/s41467-018-06449-x.

[29] B.S. Thawkar, G. Kaur, Inhibitors of NF-kappaB and P2X7/NLRP3/Caspase 1 pathway in microglia: Novel therapeutic opportunities in neuroinflammation induced early-stage Alzheimer's disease, J Neuroimmunol, 326 (2019) 62-74. https://doi.org/10.1016/j.jneuroim.2018.11.010.

[30] M. Fan, C. Wang, X. Zhao, et al., Parthenolide alleviates microglia-mediated neuroinflammation via MAPK/TRIM31/NLRP3 signaling to ameliorate cognitive disorder, Int Immunopharmacol, 120 (2023) 110287. https://doi.org/10.1016/j.intimp.2023.110287.

[31] K.W. Jo, D. Lee, D.G. Cha, et al., Gossypetin ameliorates 5xFAD spatial learning and memory through enhanced phagocytosis against Abeta, Alzheimers Res Ther, 14 (2022) 158. https://doi.org/10.1186/s13195-022-01096-3.

[32] M. Gong, X. Zhuo, A. Ma, STAT6 Upregulation Promotes M2 Macrophage Polarization to Suppress Atherosclerosis, Med Sci Monit Basic Res, 23 (2017) 240-9. https://doi.org/10.12659/msmbr.904014.

[33] R.E. Mitchell, M. Hassan, B.R. Burton, et al., IL-4 enhances IL-10 production in Th1 cells: implications for Th1 and Th2 regulation, Sci Rep, 7 (2017) 11315. https://doi.org/10.1038/s41598-017-11803-y.

[34] Y.C. Koh, G. Yang, C.S. Lai, et al., Chemopreventive Effects of Phytochemicals and Medicines on M1/M2 Polarized Macrophage Role in Inflammation-Related Diseases, Int J Mol Sci, 19 (2018) https://doi.org/10.3390/ijms19082208.

[35] Y. He, Y. Gao, Q. Zhang, et al., IL-4 Switches Microglia/macrophage M1/M2 Polarization and Alleviates Neurological Damage by Modulating the JAK1/STAT6 Pathway Following ICH, Neuroscience, 437 (2020) 161-71. https://doi.org/10.1016/j.neuroscience.2020.03.008.

[36] X. Yang, S. Xu, Y. Qian, et al., Resveratrol regulates microglia M1/M2 polarization via PGC-1alpha in conditions of neuroinflammatory injury, Brain Behav Immun, 64 (2017) 162-72. https://doi.org/10.1016/j.bbi.2017.03.003.

[37] Y. Liu, Y. Dai, Q. Li, et al., Beta-amyloid activates NLRP3 inflammasome via TLR4 in mouse microglia, Neurosci Lett, 736 (2020) 135279. https://doi.org/10.1016/j.neulet.2020.135279.

[38] I. Olsen, S.K. Singhrao, Inflammasome Involvement in Alzheimer's Disease, J Alzheimers Dis, 54 (2016) 45-53. https://doi.org/10.3233/JAD-160197.

[39] J.B. Lee, C. Adrower, C. Qin, et al., Development of Cordycepin Formulations for Preclinical and Clinical Studies, AAPS PharmSciTech, 18 (2017) 3219-26. https://doi.org/10.1208/s12249-017-0795-0.

[40] D. Ju, W. Zhang, J. Yan, et al., Chemical perturbations reveal that RUVBL2 regulates the circadian phase in mammals, Sci Transl Med, 12 (2020) https://doi.org/10.1126/scitranslmed.aba0769.

[41] M. Chen, J. Luo, W. Jiang, et al., Cordycepin: A review of strategies to improve the bioavailability and efficacy, Phytother Res, 37 (2023) 3839-58. https://doi.org/10.1002/ptr.7921.

[42] L. Ma, S. Zhang, M. Du, Cordycepin from Cordyceps militaris prevents hyperglycemia in alloxan-induced diabetic mice, Nutr Res, 35 (2015) 431-9. https://doi.org/10.1016/j.nutres.2015.04.011.